

1. Ground-based measurements

1.1. Measurements of Sun IR spectra by Brucker 125HR

Table. 1.1. Trace gases, spectral windows, degree of freedom (DOFS), errors.

N	Gas	spectral windows, cm ⁻¹	DOFS	Errors (random and systematic), %
1	H_2O	5 channels in the 1098—1222 range	1.7±0.1	0.9±0.3/—/2.3±0.2
		12 channels in the 2610—3052 range	1.9±0.1	0.4±0.2/—/2.0±0.1
2	H_2^{18}O	12 channels in the 2610—3052 range	0.8±0.1	—
3	HDO	12 channels in the 2610—3052 range	2.4±0.2	—
4	*CH ₄	2613.70—2615.40, 2650.60—2651.30, 2835.50—2835.80, 2903.60—2904.03	2.6	1.1 / 0.6 / 3.6
5	*N ₂ O	2481.30—2482.60, 2526.40—2528.20, 2537.85—2538.80, 2540.10—2540.70	3.6	1.3 / 0.2 / 2.6
6	*CO	2057.70—2058.00, 2069.56—2069.76, 2157.50—2159.15	2.5	1.0 / 0.1 / 1.7
7	CO ₂	2620.55—2621.10, 2626.40—2626.85, 2627.10—2627.60, 2629.275—2629.95	1.0	0.9 / 2.2 / 3.1
8	*C ₂ H ₆	2976.66—2976.95, 2983.20—2983.55	1.2	3.3 / 2.0 / 3.5
9	*HCN	3268.05—3268.35, 3331.40—3331.80	1.6	14 / 7.3 / 5.2

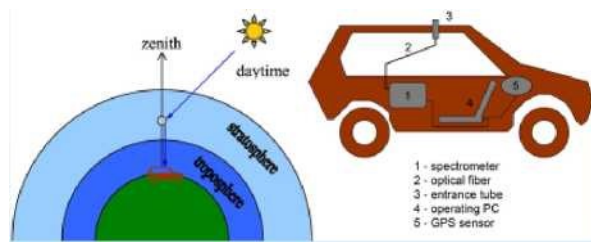
10	H ₂ CO	2763.42—2764.17, 2765.65—2766.01, 2778.15—2779.10, 2780.65—2782.00	1.4	5.0 / 4.5 / 14
11	OCS	2030.75—2031.06, 2047.85—2048.24, 2049.77—2050.18, 2051.18—2051.46, 2054.33—2054.67	2.6	1.7 / 1.1 / 3.4
12	NH ₃	929.40—931.40, 962.10—970.00	1.0	12 / 2.6 / 21
13	CFC-11	830 — 860	1.3±0.2	3.9±0.7/0.2±0.01/7.6±0.2
14	CFC-12	1160—1162	1.7±0.07	3.5±0.8/0.8+0.3/3.2±0.4
15	HCFC-22	828.75 829.4	1.1±0.4	3.6±0.9/2.2±1.3/4.9±0.7
16	*O ₃	991.25—993.80, 1001.47—1003.04 1005.00—1006.90, 1007.35—1009.00	4.1±0.2	1.9±0.3/—/2.1±0.1
17	¹⁶ O ¹⁶ O ¹⁸ O	13 channels in the 960—1045 range	1.0±0.2	-
18	¹⁶ O ¹⁸ O ¹⁶ O	13 channels in the 960—1045 range	0.9±0.2	-
19	*HCl	2727.73—2727.83, 2775.70—2775.80, 2925.80—2926.0	2.5±0.2	2.3±0.7/1.1±0.2/5.1±0.9
20	*HF	4038.81—4039.07	2.6±0.2	2.1±0.6/0.7±0.3/5.6±0.1
21	*HNO ₃	866.5—875.2	2.8±0.4	4.6±2.0/—/11.0±0.8
22	*ClONO ₂	779.00—782.38, 779.90—780.32	1	14±6/—/15±5 (from December to April)
23	NO ₂	2914.6—2914.7	1.2±0.1	9±2/8±2/9±1
24	C ₂ H ₂	3250.25—3251.11	1.0	32/7/22
25	HCOOH	1104.65—1105.60	1.0	12/0.5/21

1.2. Stationary and Mobile DOAS O₃ and NO₂ measurements

St.Petersburg State University

Schematic instrument set-up and specifications of mobile DOAS zenith-sky observations
based on commercial spectrometer OceanOptics HR4000

Spectrometer design	asymmetric cross-Oemly-Turner
Light detector	3MB-element CCD (Toshiba TCD1304AP)
Analog-to-digital converter resolution	14-bit
Entry slit width	50 nm
Input focal length	P/4 101 mm
Input fiber bundle	600 nm diameter, 2 m length
Field-of-view	25°
Spectral range	400-610 nm
Spectral resolution	0.6 nm (FWHM)



- 24/06/2015

Page 29 —

Fig.1.1. Scheme and specifications of mobile DOAS observations

St.Petersburg State University

The track of mobile DOAS measurements on 14/08/2012. The circular arrows show the driving direction the track starts at point "A" and ends at point "B" after the full loop, plus recurrent track "AB" (the color pattern shows NO₂ column, 10¹⁵ molecules/cm²). The blue arrow show the wind direction.



Fig. 1.2. Track of mobile DOAS measurements (from "A" to "B")

Average annual NOx emission rate for SPb - 55 kT/year

Ionov D., A. Poberovskii, 2018: Observations of urban NOx plume dispersion using the mobile and satellite DOAS measurements around the megacity of St.Petersburg (Russia). *International Journal of Remote Sensing*, doi: DOI: 10.1080/01431161.2018.1519274.

1.3. In situ measurements near-ground concentration of CO₂, CH₄, H₂O, O₃ and etc.

Gas analyzer Los Gatos Research GGA 24r-EP was used for measuring the volume mixing ratio (vmr) of CH₄, CO₂ and H₂O. Gas analyzer Los Gatos Research CO 23r was used for measuring the CO and H₂O vmr. The concentration of NO and NO₂ (NOx) was measured by gas analyzer ThermoScientific 42i-TL.

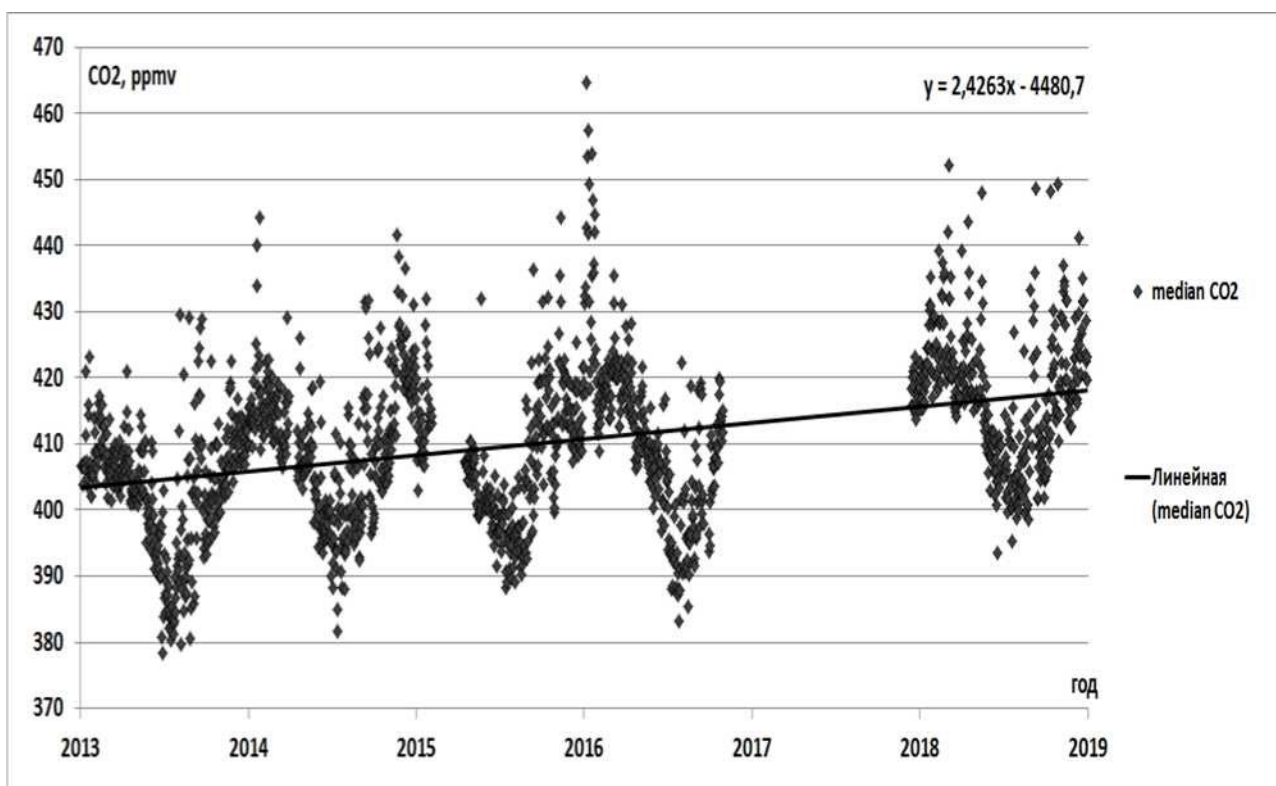


Fig. 1.3. Median CO₂ daily concentration (2013-2018).

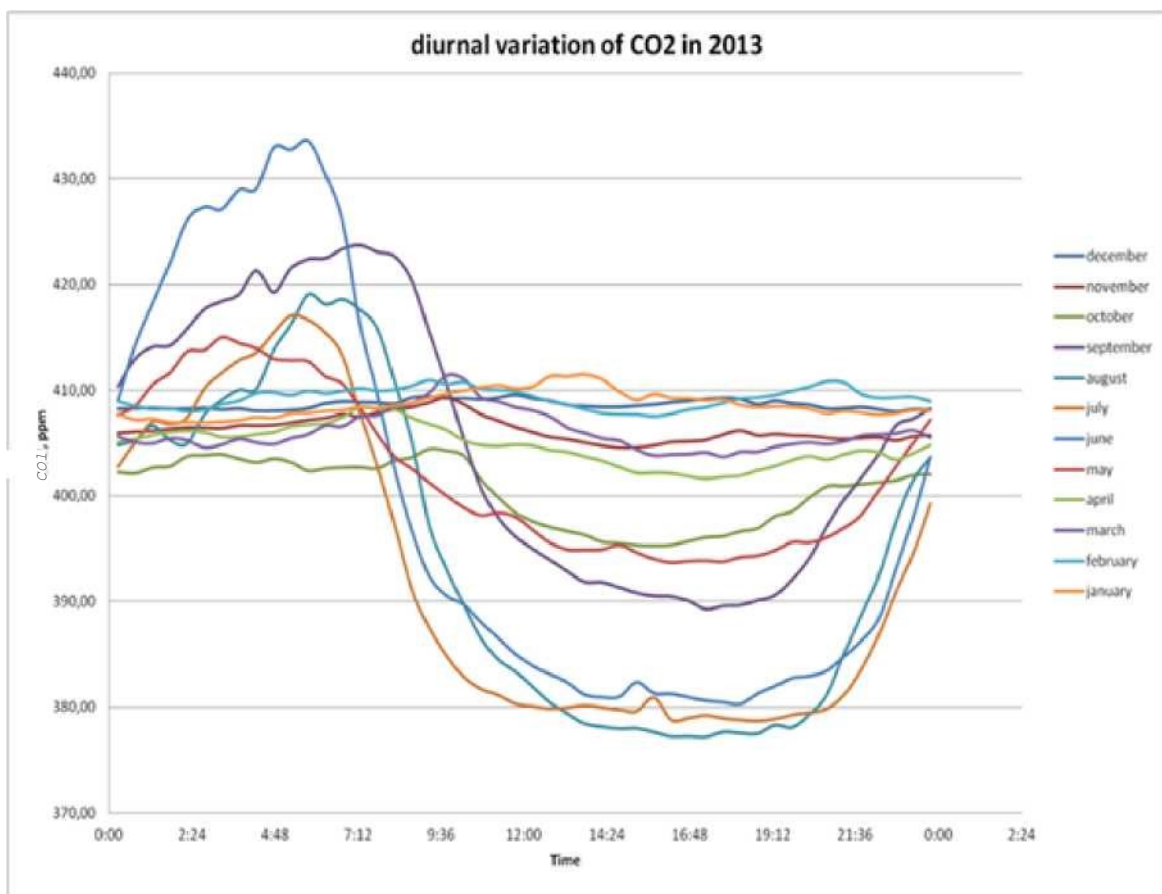


Fig. 1.4. Diurnal CO₂ variations in 2013.

1.4. Trends of total columns of trace gases (Bruker 125HR)

Table 1.2. Trends of trace gases - Saint-Petersburg

Gas	Error, %	Trends in Peterhof, per year	Independent trend estimates, per year
CO ₂	0.4-0.6	0.52±0.02 %, ~2.0 ppm	1.62-2.86 ppm
CH ₄	0.5-1.0	0.42±0.02 %	6.9-7.6 ppb, 0.38 %
N ₂ O	1-2	0.28±0.02 %	0.74-0.93 ppb, 0.270.32%
O ₃ (0-8 km)	1-2	-0.75±0.56 %, -0.22±0.17 DU	from -0.31 to +0.16 DU
CFC-11	3.9	-0.69±0.11 %	-(0.6-0.9) %
CFC-12	3.5	-0.42±0.06 %	-(0.4-0.76) %
HCFC-22	3.6	2.24±0.18 %	2.7-3.5 %
HF	2-3	0.6±0.4 %	from -1.11 to +1.61% 4.97 % (1991-1997), 1.12 % (1998-2005)
ClONO ₂	14-19	-2.0±1.6 %	from -4.56 to +6.79 %

Timofeev, Y.M., Polyakov, A.V., Virolainen, Y.A. et al. Estimates of Trends of Climatically Important Atmospheric Gases near St. Petersburg. *Izv. Atmos. Ocean. Phys.* 56, 79-84 (2020).
<https://doi.org/10.1134/S0001433820010119>

1.5. Comparison of experimental and modeled spatial and temporal variations of trace gases (together with Prof. S.P. Smyshlyaev and O. Kirner)

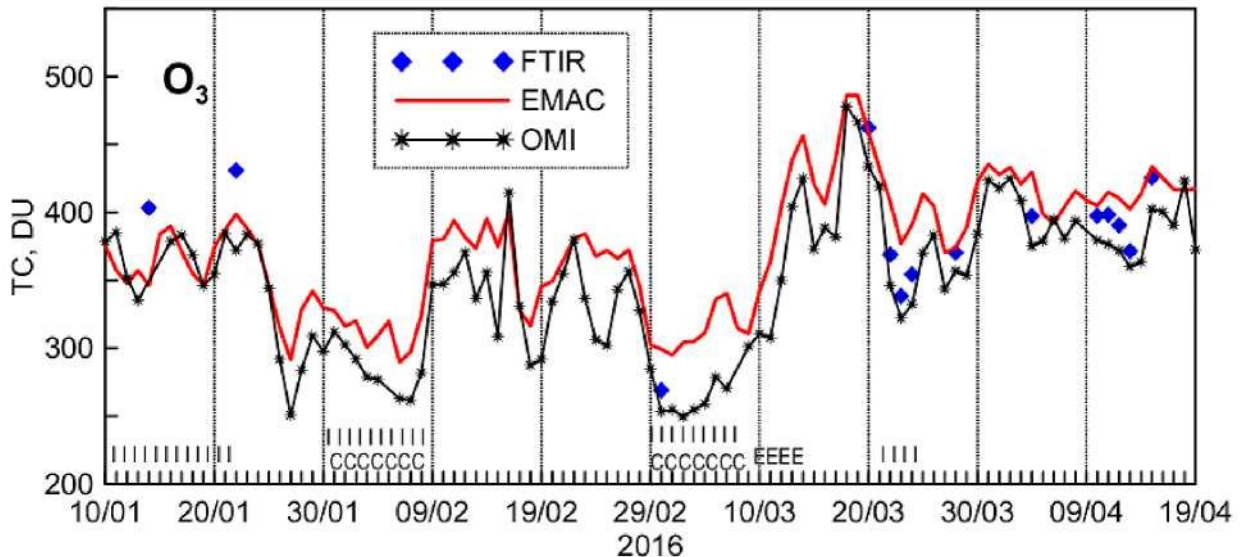


Fig. 1.5. Variations of O₃ total column from ground-based (FTIR), satellite (OMI) measurements and modeling study (EMAC).

Shved G.M., Ya.A. Virolainen, Yu.M. Timofeyev, S.I. Ermolenko, S.P. Smyshlyaev, M.A. Motsakov, and O. Kirner, 2018: Ozone Temporal Variability in the Subarctic Region: Comparison of Satellite Measurements with Numerical Simulations. *Izvestiya, Atmospheric and Oceanic Physics*, 54, 1, 32-38. DOI: 10.1134/S0001433817060111

Virolainen Ya.A., Yu.M. Timofeev, I.A. Berezin, S.P. Smyshlyaev, M.A. Motsakov, and O. Kirner, 2018: Validation of Atmospheric Numerical Models Based on Satellite Measurements of Ozone Columns. *Russian Meteorology and Hydrology*, 3, 161-167. DOI: 10.3103/S1068373918030044.

Cherepova M.V., S.P. Smyshlyaev, M.V. Makarova, Yu.M. Timofeyev, A.V. Poberovskiy, and G.M. Shved, 2018: A Study of the Column Methane ShortTerm Variability in the Atmosphere on a Regional Scale. *Izvestiya, Atmospheric and Oceanic Physics*, 54, 5, 558-569. DOI: 10.1134/S0001433818060038.

Smyshlyaev S.P., Ya.A. Virolainen, M.A. Motsakov, Yu.M. Timofeyev, A.V. Poberovskii, A.V. Polyakov, 2017: Interannual and seasonal variations in ozone in different atmospheric layers over St. Petersburg based on observational data and numerical modeling. *Izvestiya, Atmospheric and Oceanic Physics*, 53, 3, 301-315. DOI: 10.1134/S0001433817030148.

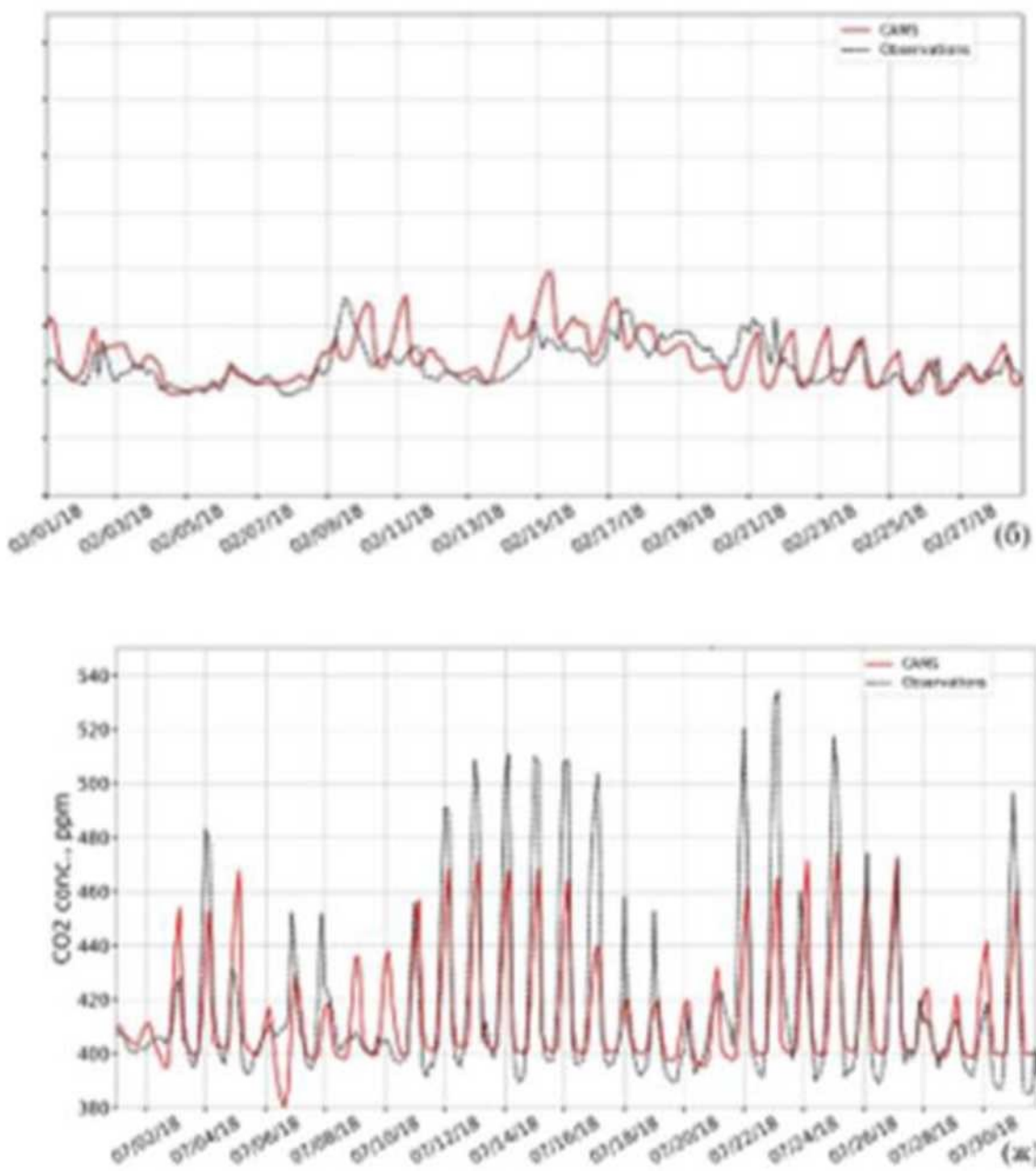


Fig. 1.6. Comparison of CAMS (Copernicus Atmosphere Monitoring Service) forecast and in situ CO₂ measurements (2018).

Nerobelov et al. Comparison of CAMS forecast and CO₂ measured near Saint-Petersburg. Optics of atmosphere and ocean (in press).

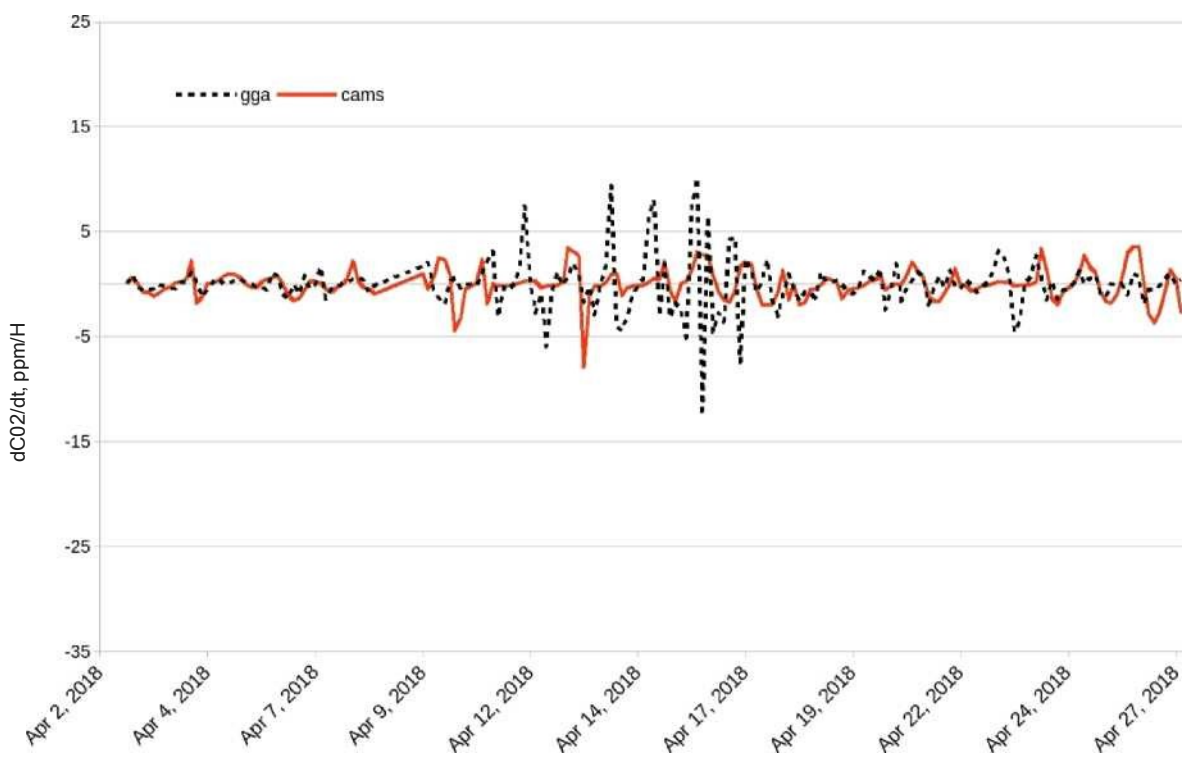


Fig. 1.7. Comparison of modeled and measured CO₂ gradient concentrations near Saint-Petersburg (ppm/hours).

C1ONO₂

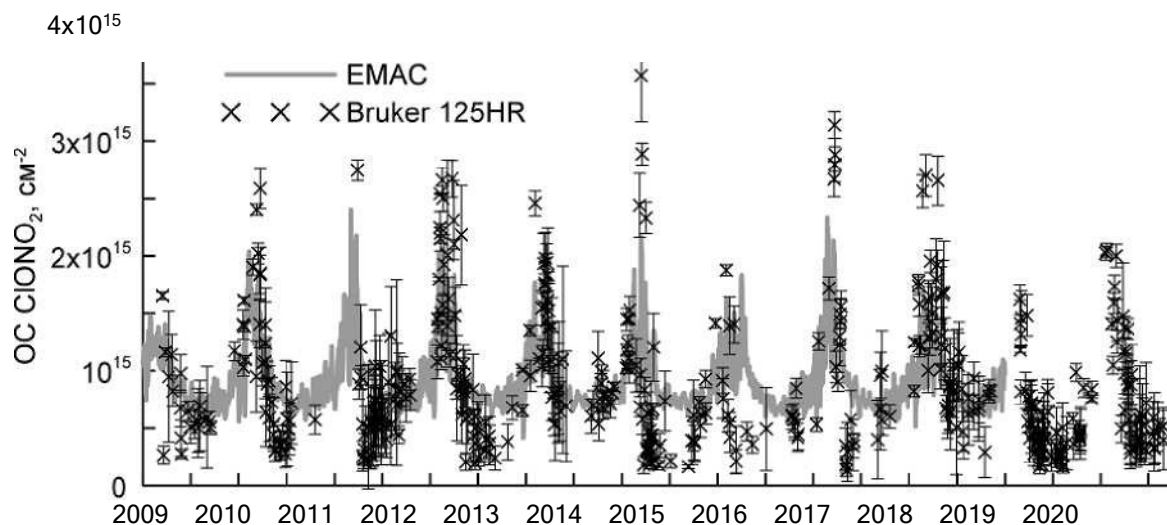


Fig. 1.8. Comparison of modeled and measured the total C1ONO₂ contents near Saint-Petersburg (cm⁻²).

Results of retrieving the total C1ONO₂ content from the spectra measured using the Bruker 125HR Fourier spectrometer at the NDACC site St. Petersburg in the period from 2009 to 2019 were compared with the calculations by the EMAC chemistry-climate model. For the period 2009–2017, the average mismatch between the model and experimental ensembles was 3%, the standard deviation was 43%, and the correlation coefficient was 0.79 ± 0.02 , which indicates an adequate description of the variability of the total C1ONO₂ content by the model. The assessment of the linear trend of the total C1ONO₂ content showed a significant decrease in the total chlorine nitrate content in the atmosphere over St. Petersburg both according to ground-based measurements ($-2.3 \pm 1.9\%$ per year) and modeling results ($1.2 \pm 0.4\%$ per year).

Y. A. Virolainen, A. V. Polyakov, O. Kirner. Optimization of determining chlorine nitrate in the atmosphere from ground-based spectroscopic measurements // *J. Appl. Spectrosc.* 87. N 2. 2020 (in print).

1.6. Ozone mini hole (2016) numerical modeling

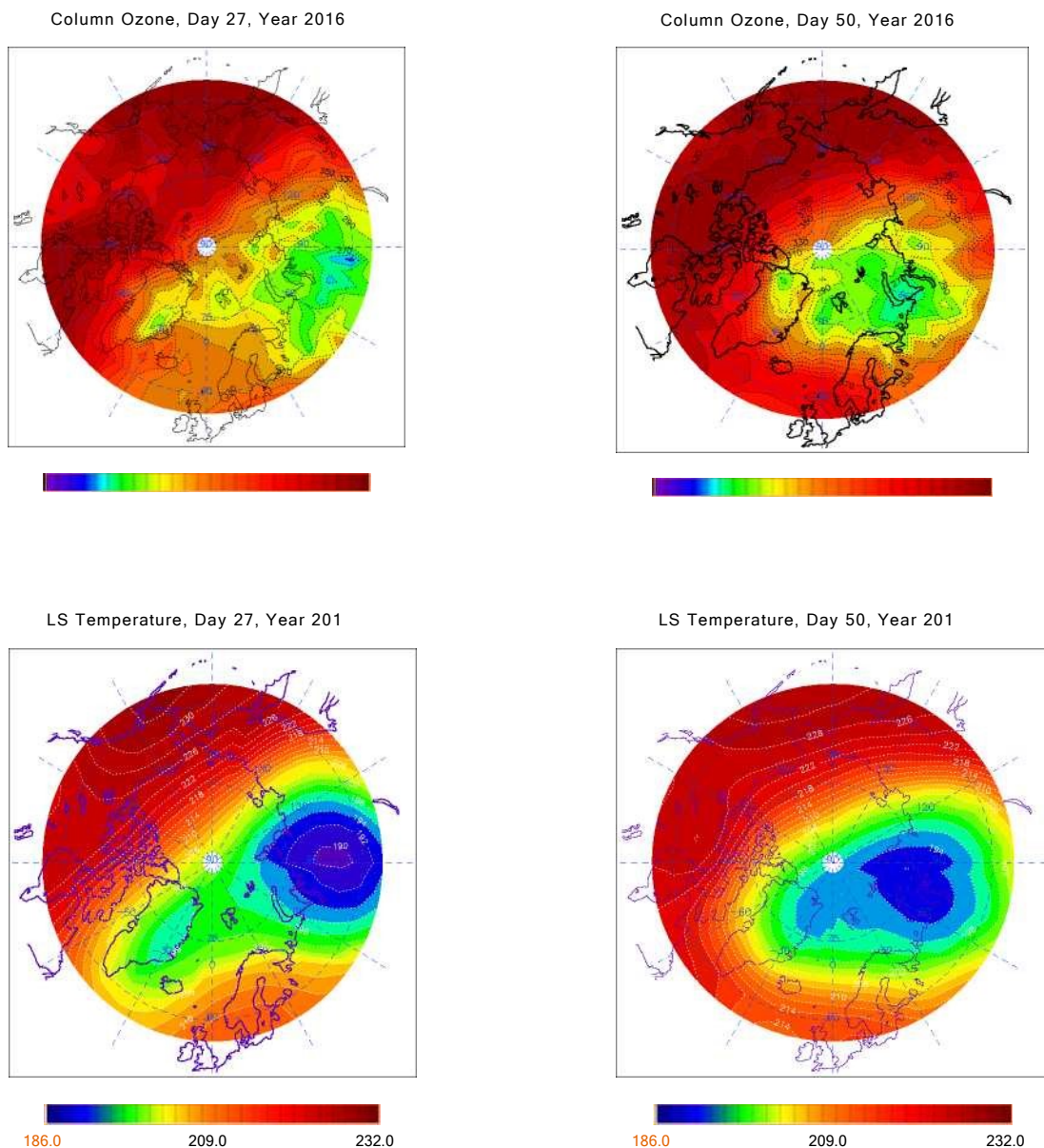


Fig. 1.9. Column ozone (Dobson units) for days with minimum local registered values (*top panels*) and temperature of the lower stratosphere (K) for the same days (*bottom panels*) simulated with the RSHU model.

Timofeyev, Y. M., Smyshlyaev, S. P., Virolainen, Y. A., Garkusha, A. S., Polyakov, A. V., Motsakov, M. A., and Kirner, O., 2018: Case study of ozone anomalies over northern Russia in the 2015/2016 winter: Measurements and numerical modeling. *Ann. Geophys.*, 2028, 36, 6, 1495-1505.

Chubarova N.E., Yu.M. Timofeev, Ya.A. Virolainen & A.V. Polyakov, 2019: Estimates of UV Indices During the Periods of Reduced Ozone Content over Siberia in Winter-Spring 2016 . *Atmospheric and Oceanic Optics*, 32, 2, 177-179.
DOI:10.1134/S1024856019020040.

1.7. Estimation of trace gas emission by local and remote measurements (together with German colleagues)

The concept of EMME is based on remote measurements of the total column amount of CO₂, CH₄ and CO from two mobile platforms located inside and outside the city plume combined with the mobile circular measurements of tropospheric column amount of NO₂ from the third nonstop moving platform, the latter measurements are used for the realtime control of the megacity plume evolution.

The mean CO₂ emission flux for St. Petersburg as an area source was estimated as **89±28 kt*km⁻²*yr⁻¹ (45-130 variation), which is two times higher** than the corresponding value in the EDGAR database. The experiment revealed the **CH₄ emission flux of 135±68 t*km⁻²*yr⁻¹ which is about one order of magnitude greater** than the value reported by the official inventories of St. Petersburg emissions (~ 17 t km⁻² yr⁻¹ for 2017). At the same time, for the urban territory of St. Petersburg, both the EMME experiment and the official inventories for 2017 give **similar results for the CO anthropogenic flux (251±104 t*km⁻²*yr⁻¹ vs. 280 t*km⁻²*yr⁻¹) and for the NOx anthropogenic flux (66±28 t*km⁻²*yr⁻¹ vs. 47 t*km⁻²*yr⁻¹).**

spectral resolution: 0.5 cm⁻¹
spectral range 5000 - 1,2000 cm⁻¹, 4000
12000 cm⁻¹ (option)
dimensions: approx. 470 x 630 x 350 mm
mass: kg

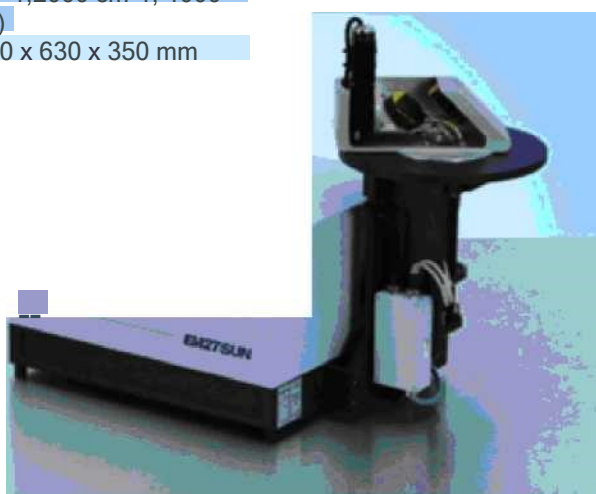


Fig. 1.10. Compact spectrometer for atmospheric measurements by solar absorption spectroscopy EM27/SUN.

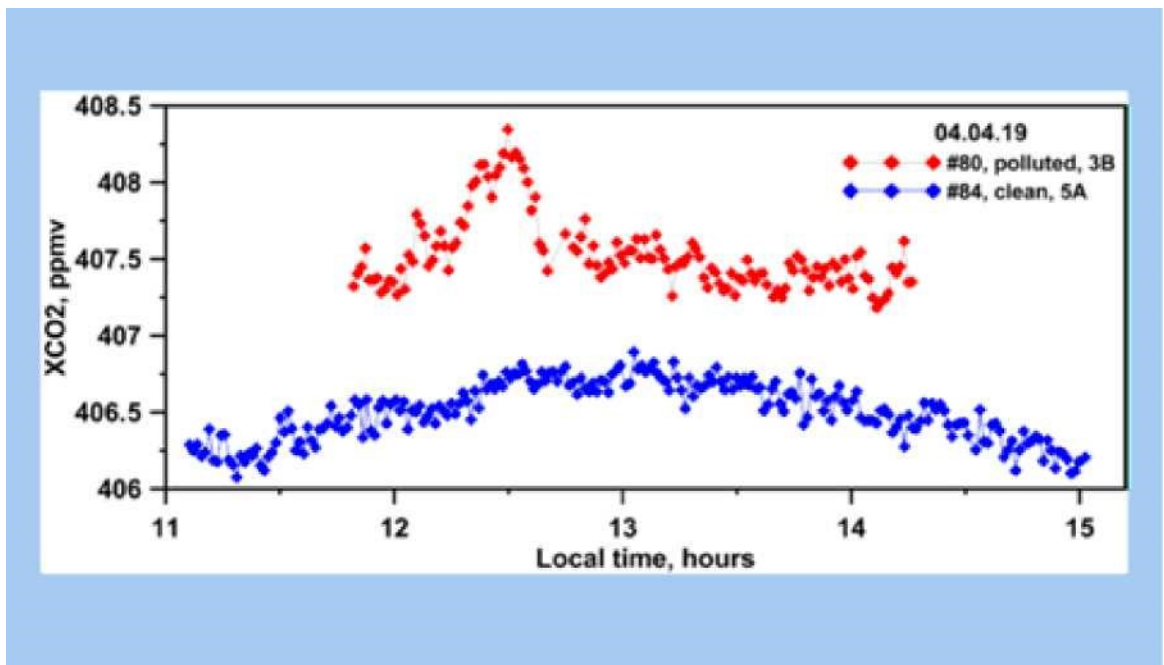


Fig. 1.11. Spectroscopic measurements of XCO₂ in clean and polluted air near St. Petersburg.

Maria V. Makarova, Carlos Alberti, Dmitry V. Ionov, Frank Hase, Stefani C. Foka, Thomas Blumenstock, Thorsten Warneke, Yana A. Virolainen, Vladimir S. Kostsov, Matthias Frey, Anatoly V. Poberovskii, Yuri M. Timofeyev, Nina N. Paramonova, Kristina A. Volkova, Nikita A. Zaitsev, Egor Y. Biryukov, Sergey I. Osipov, Boris K. Makarov, Alexander V. Polyakov, Viktor M. Ivakhov, Hamud Kh. Imhasin, Eugene F. Mikhailov. Emission Monitoring Mobile Experiment (EMME): an overview and first results of the St. Petersburg megacity campaign-2019 // *AMT Journal*, <https://doi.org/10.5194/amt-2020-87>.

Table 1.3. Estimates of anthropogenic CO₂ emissions from Saint-Petersburg megacity. (Timofeev Yu. M., Nerobelov G.M., Poberovsky A.V., Foka S.)

Sources	Emission MtCO ₂ /year
Emission Monitoring Mobile Experiment (EMME), City - 1427 km ²	65.4 (2019)
Emission Monitoring Mobile Experiment (EMME), Center part - 394 km ²	39.9 (2019)
ODIAC, city	33.8 (2018)
CAMS, city	66.8 (2018)
OCO-2	39.2 (2016, 2018)
Inventory	30.0 (2018)

1.8. MW atmospheric and cloud sounding

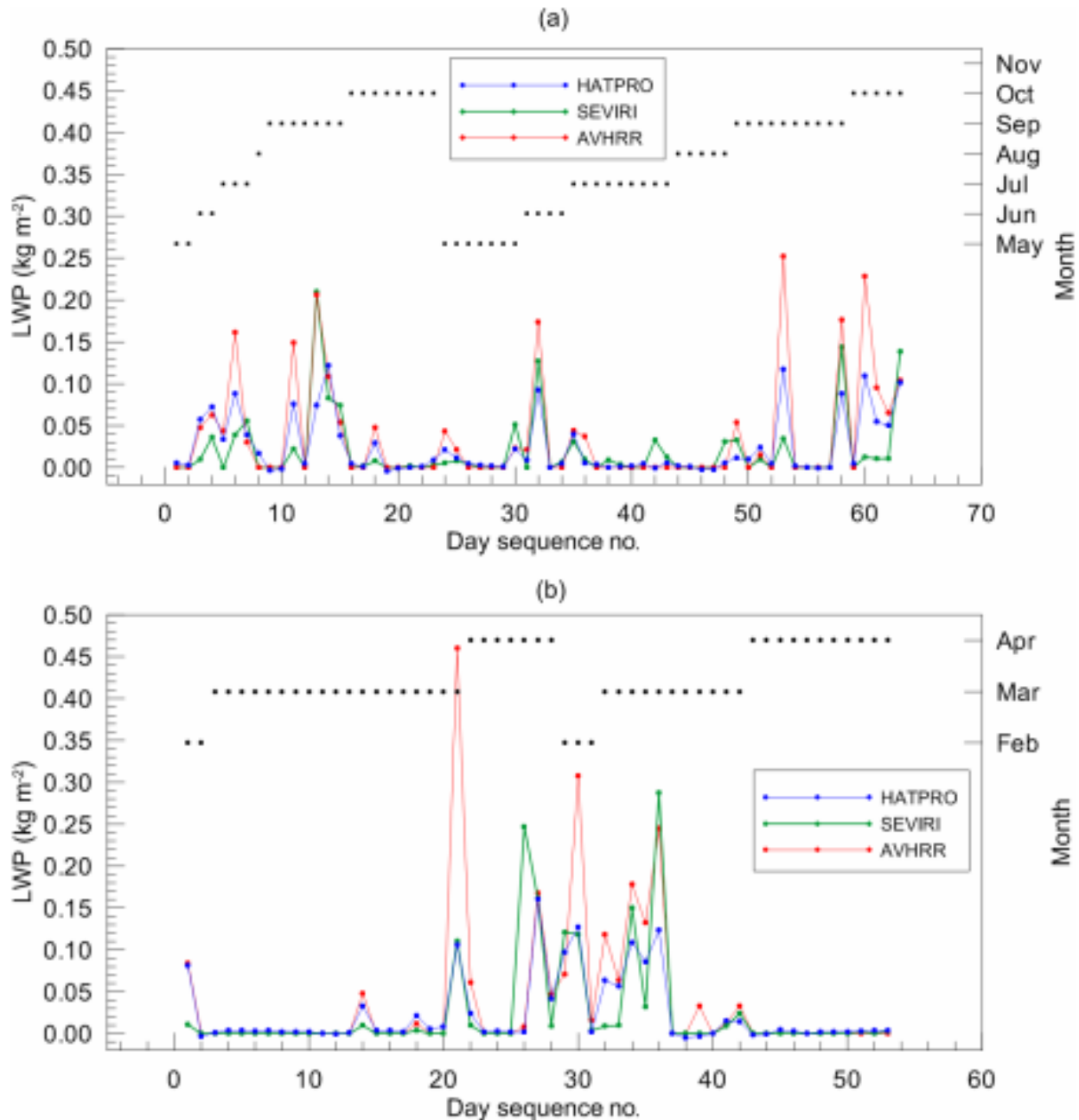


Fig. 1.12. The LWP values obtained by HATPRO (HAT60, blue dots), SEVIRI (green dots), and AVHRR (red dots) as a function of day sequence number for the WH and CD seasons (a and b respectively).

Kostsov V.S. , Kniffka A., Stenge M., Ionov D.V. , 2019: Cross-comparison of cloud liquid water path derived from observations by two space-borne and one ground-based instrument in Northern Europe. *Atm. Measurement Techn.*, 12, 5927-5946, <https://doi.org/10.5194/amt-12-5927-2019>.

1.9. Comparison of different remote sensing methods (water vapour)

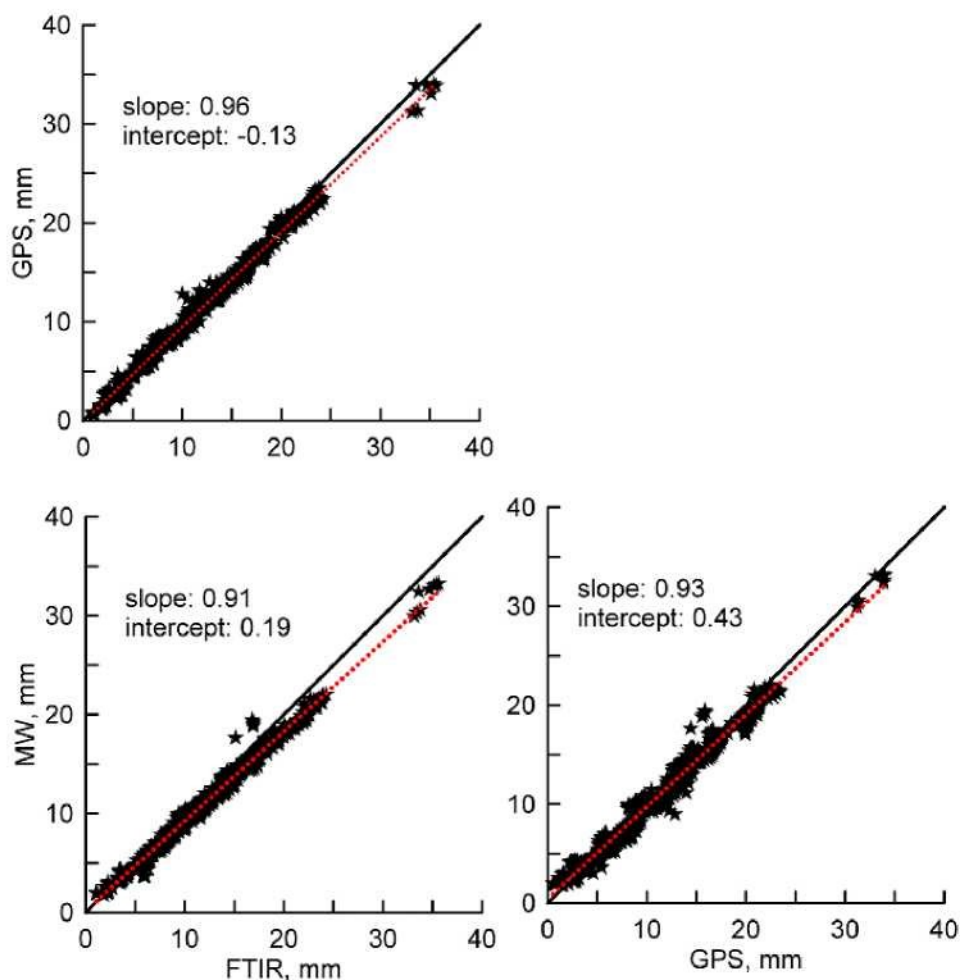


Fig. 1.13. Intercomparison of integrated water vapor (IWV) values measured by Bruker 125 HR (FTIR), microwave radiometer RPG-HATPRO (MW) and global navigation satellite system receiver Novatel ProPak-V3 (GPS) at the St. Petersburg site.

It is shown that GPS and MW data quality depends on the atmospheric conditions; in dry atmosphere, these techniques are less reliable at the St. Petersburg site than the FTIR method. We evaluate the upper bound of statistical measurement errors for clear-sky conditions as 0.29 ± 0.02 mm ($1.6 \pm 0.3\%$), 0.55 ± 0.02 mm ($4.7 \pm 0.4\%$), and 0.76 ± 0.04 mm ($6.3 \pm 0.8\%$) for FTIR, GPS and MW methods, respectively. We proposed to use FTIR as a reference method under clear-sky conditions since it is reliable on all scales of IWV variability.

Virolainen, Y. A., Timofeyev, Y. M., Kostsov, V. S.; et al. Quality assessment of integrated water vapour measurements at the St. Petersburg site, Russia: FTIR vs. MW and GPS techniques // Atmos. Meas. Tech., 10, 4521-4536, 2017 <https://doi.org/10.5194/amt-10-4521-2017>

2. Satellite measurements and analysis

2.1. Methods, algorithms and software for interpretation of IKFS-2 and MW spectrometers (Meteor satellite)

2.1.1. Satellite temperature sounding

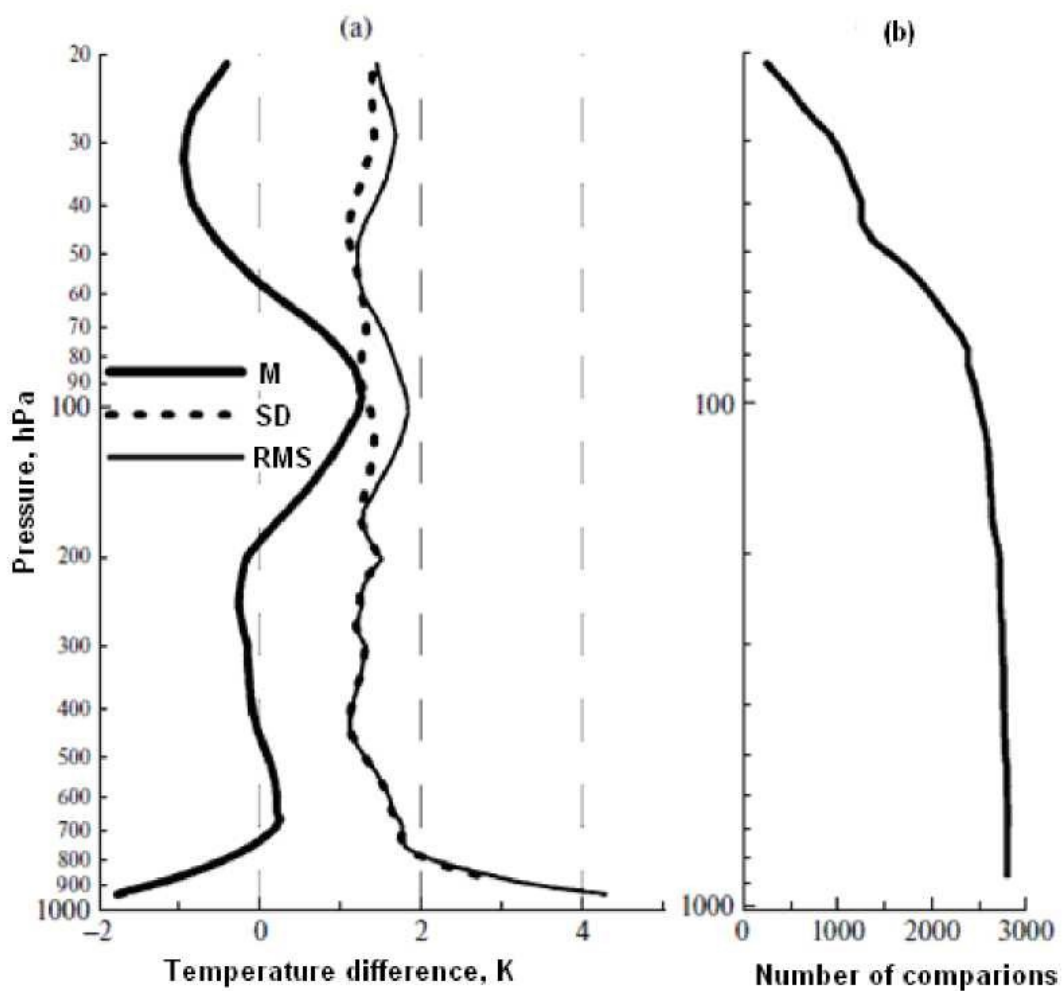


Fig. 2.1. Mean (M), root-mean square (RMS) and standard difference (SD) between IKFS-2 temperature retrieval and radiosonde measurements (a) and number of comparisons (b).

Timofeyev Yu.M., A.B. Uspensky, F. S. Zavelevich, A. V. Polyakov, Y. A. Virolainen, A. N. Rublev, A. V. Kukharsky, J. V. Kiseleva, D. A. Kozlov, I.A. Kozlov, A.G. Nikulin, V. P. Pyatkin, E. V. Rusin, 2019: Hyperspectral infrared atmospheric sounder IKFS-2 on “Meteor-M” No. 2 - Four years in orbit. *J. Quant. Spec. Rad. Trans.*, 238, 106579, <https://doi.org/10.1016/j.jqsrt.2019.106579>

2.2. Satellite IR ozone monitoring

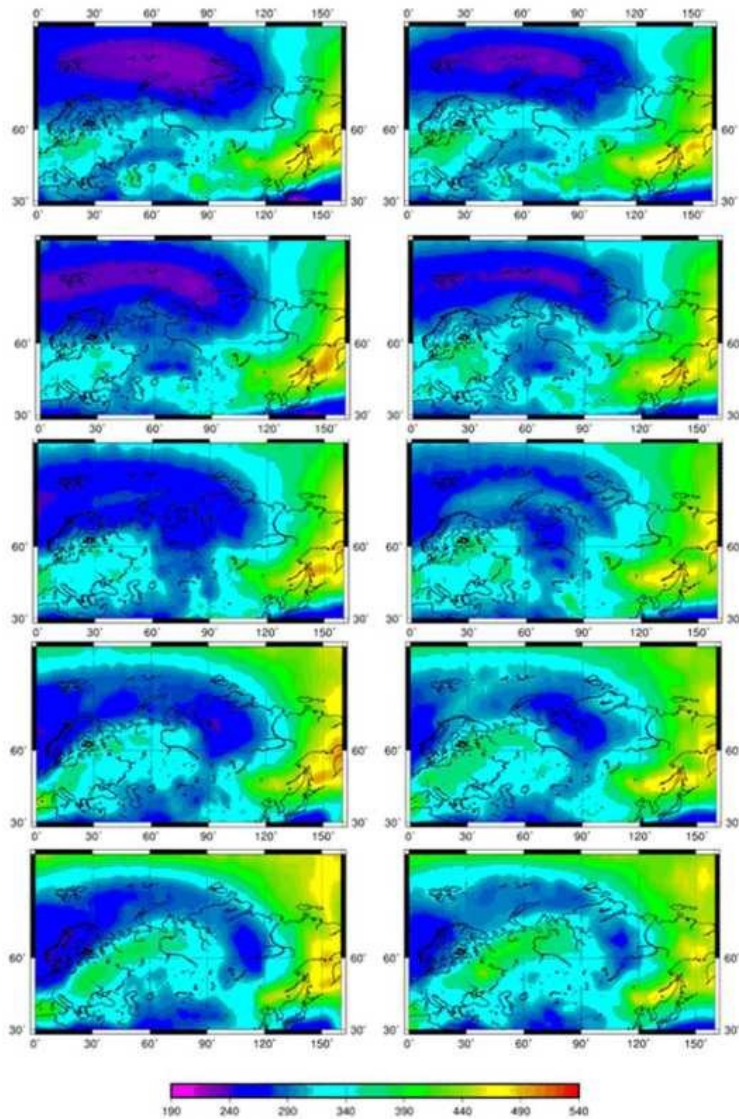


Fig. 2.2. Spatial distributions of total ozone columns on 23-27 February 2016, based on measurements of two instruments of the same type - IKFS-2 (column a) and IASI (column b) (Garkusha et al., 2018).

Yury M. Timofeyev, Sergei P. Smyshlyaev, Yana A. Virolainen, Alexander S. Garkusha, Alexander V. Polyakov, Maxim A. Motsakov, Ole Kirner. Case study of ozone anomalies over northern Russia in the 2015/2016 winter: Measurements and numerical modeling. *Ann. Geophys.*, 36, 1495-1505, 2018
<https://doi.org/10.5194/angeo-36-1495-2018>

Episodes of the extremely low ozone columns were observed over the territory of Russia in the Arctic winter of 2015/2016 and the beginning of spring 2016.

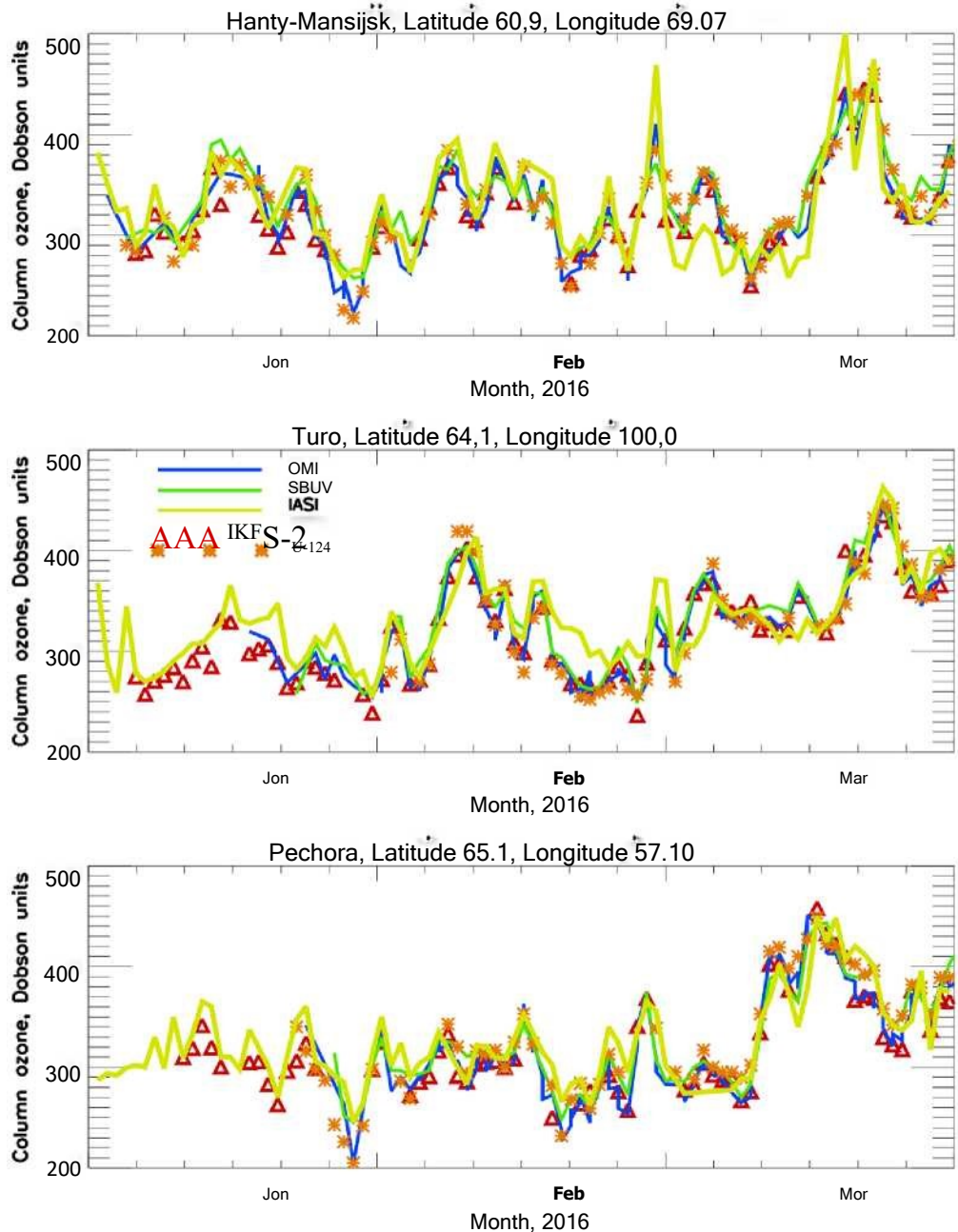


Fig. 2.3. Comparison of total ozone columns (TOCs) retrieved from different remote sensing techniques with results of the numerical modeling.

Timofeyev, Y. M., Smyshlyaev, S. P., Virolainen, Y. A. et al. Case study of ozone anomalies over northern Russia in the 2015/2016 winter: measurements and numerical modeling. *Ann. Geophys.*, 36, 1495-1505, <https://doi.org/10.5194/angeo-36-1495-2018>, 2018

New ozone hole - March - April 2020,

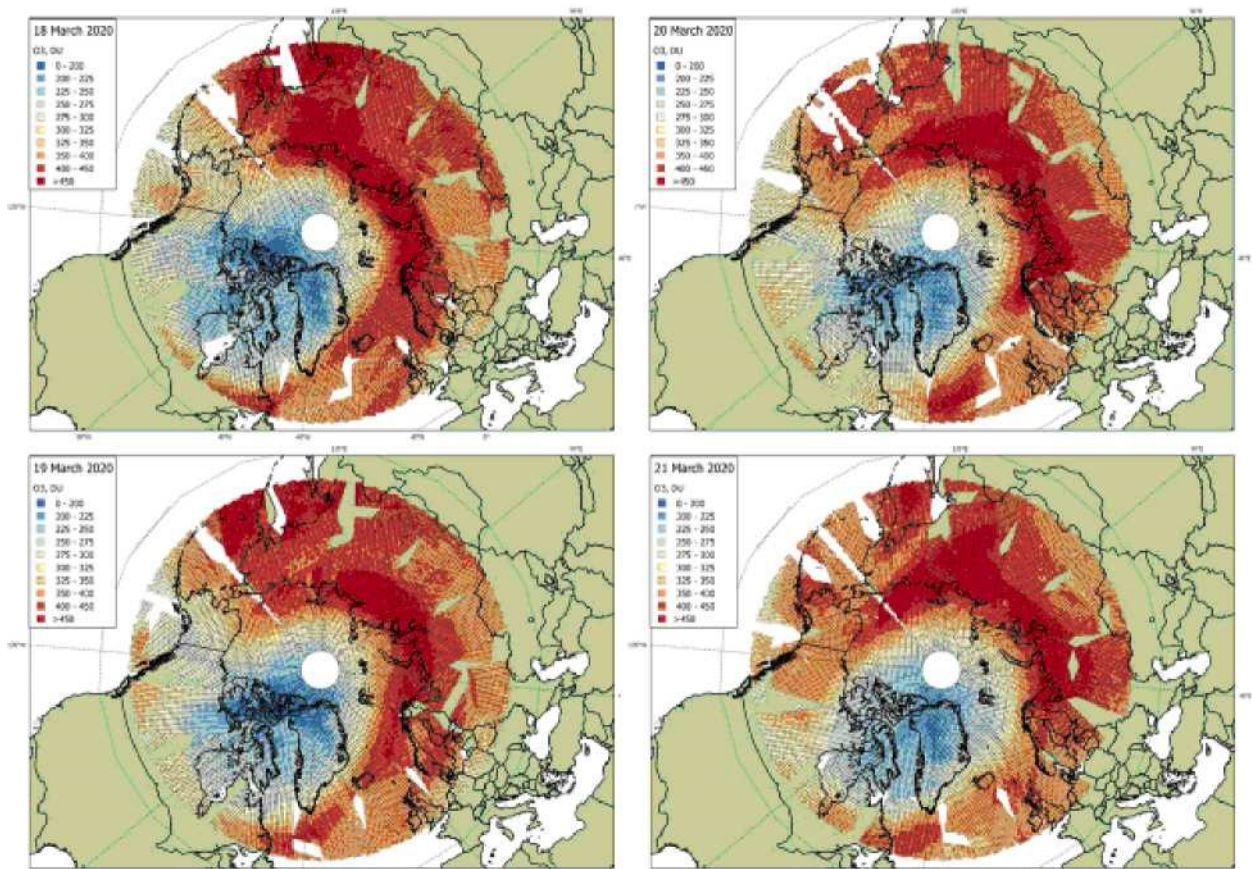


Fig. 2.4. Results of sounding the new ozone hole (March-April 2020) by Russian satellite device IKFS-2 ("Meteop-M" №2).

2.3. Climate investigation using satellite measurements

Studies of climate changes by comparing the measurements of outgoing thermal radiation in 1977 and 1979 and 2016-2018 (SI-1 and IKFS-2 devices) (together with German colleagues)

Measurements by SI-1 device - 1977-1978 and IKFS-2 device - 2015-2018

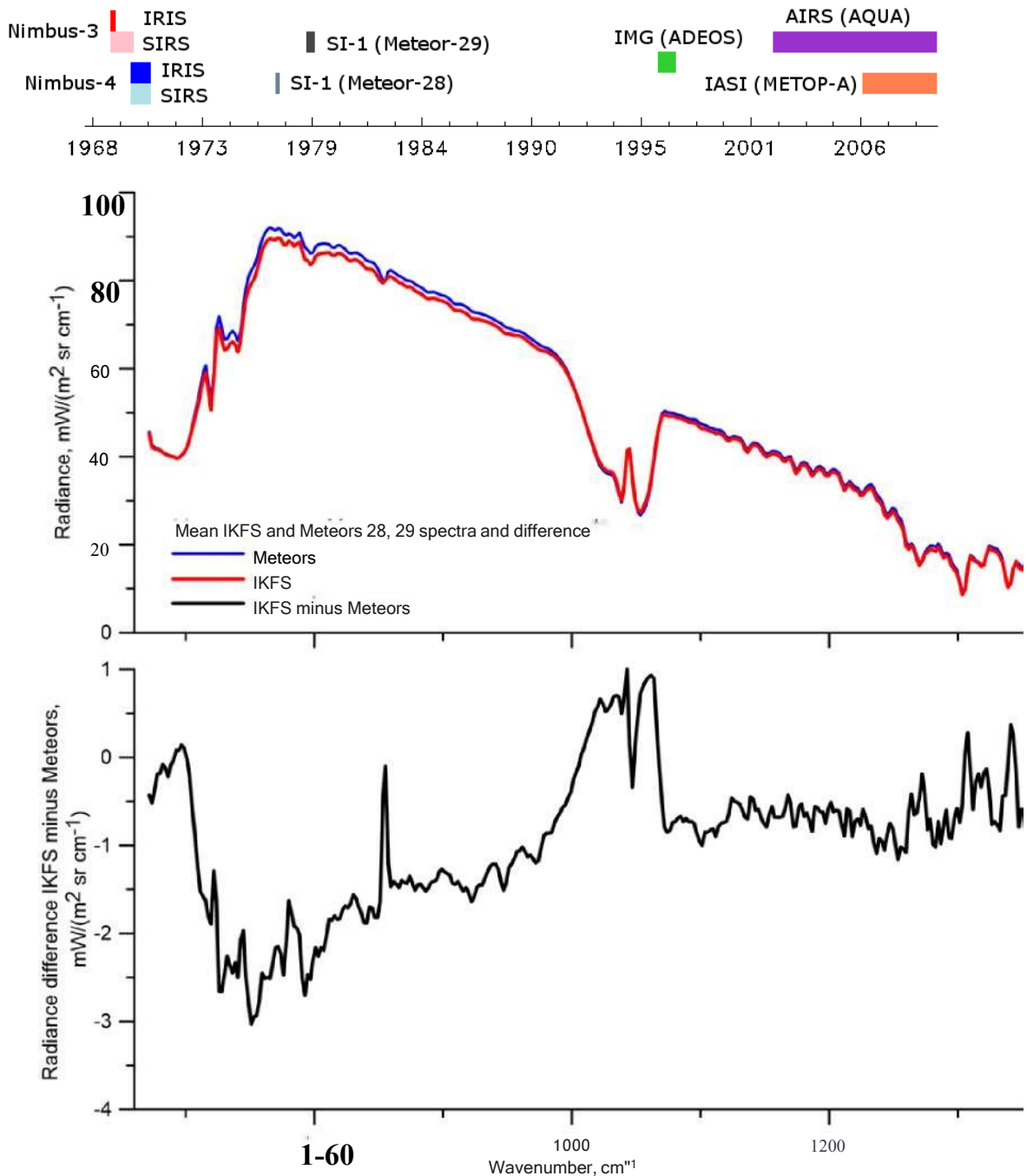


Fig. 2.5. Mean outgoing thermal radiation measured by SI-1 device - 1977-1978 and IKFS-2 device - 2015-2018 and differences.

2.4. CO₂ emission from OCO-2 measurements

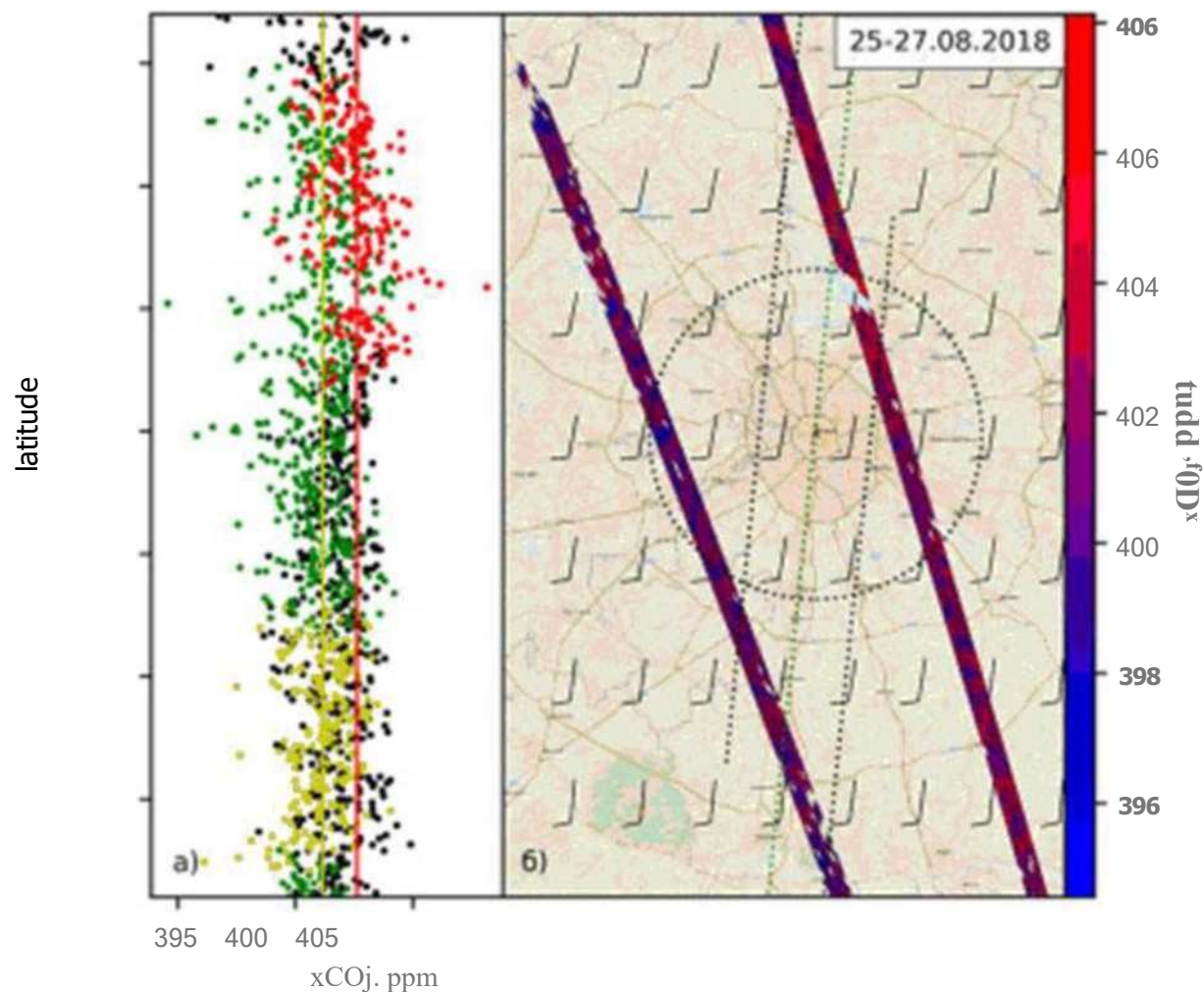


Fig. 2.6. Spatial distribution of OCO-2 XCO₂ measurements on the territory of Moscow (right) and latitudinal distribution of XCO₂ (left) in 25-27 Aug 2018.

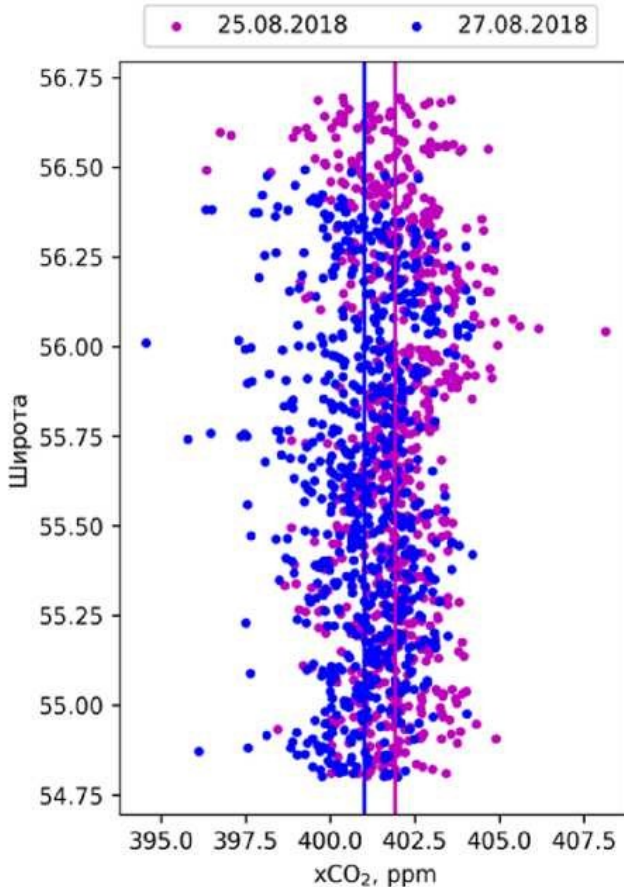


Fig. 2.7. Latitudinal distribution of XCO₂ on the territory of Moscow in 25 (pink circles) and 27 (blue circles) Aug 2018.

The rates of CO₂ anthropogenic emissions are estimated for Saint Petersburg and Moscow megacities based on satellite CO₂ measurements by OCO-2 instrument. The CO₂ emission rates for Saint Petersburg amount to 80 and 74 t/km² per day on March 1, 2016, and May 12, 2018, respectively. The CO₂ emission rate for Moscow is estimated as 123, 179, and 186 t/km² per day for August 25, 2018, June 22, 2018, and March 26, 2017, respectively. The comparison of our results with the estimates for other megacities has shown that the emission estimates for Saint Petersburg are close to those for Los Angeles and Berlin, and estimates for Moscow are close to those for London. The estimation errors are mainly caused by the anthropogenic contribution, which varies from 30% to ~90%.

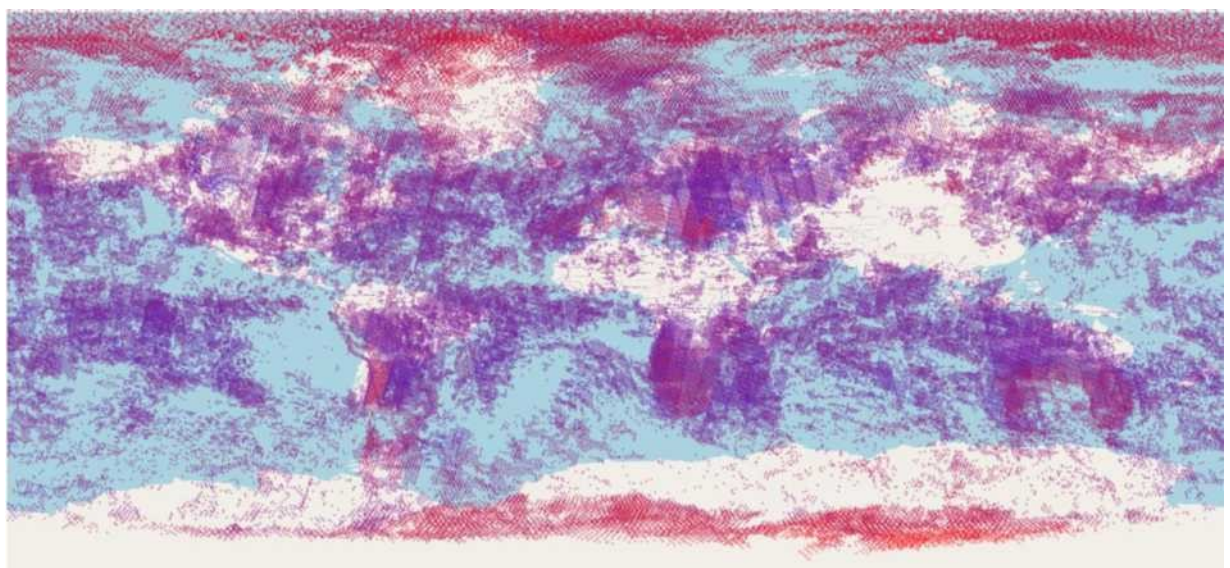
Timofeev Yu.M., Berezin I.A., Virolainen Ya.A., Poberovsky A.V., Makarova M.V., Polyakov A.V. Estimates of anthropogenic CO₂ emissions for Moscow and St. Petersburg based on OCO-2 satellite measurements. // *Optika Atmosfery i Okeana*. 2020. V. 33. No. 04. P. 261-265 [in Russian].

Important problem - validation of satellite emission estimations

Table 2.1. Saint-Petersburg anthropogenic CO₂ emissions from different sources.

Method	Emission ktCO₂/kM² for year
EMME (9 days)	92±26 (2019)
EMME (4 days)	87±14 (2019)
Local measurements	40±30 (2019)
OCO-2	27-29±10 (2019)
ODIAC (1417 km²)	23.8 (2018)
ODIAC (394 km²)	52.2 (2018)
Official monitoring 2017	22.4 (2015)

2.5. Remote sensing the CO₂ radiation forcing from Meteor satellite



- -3317 --3002
- -3002 -2686
- -2686--2370
- -2370-2055
- -2055 --1739
- -1739-1423
- -1423--1108
- -1108--792
- -792-476
- -476--161

Fig. 2.8. Radiation CO₂ forcing from "Meteop-M" N»2, (IKFS-2)

Timofeev Yu.M., Virolainen Ya.A., Polyakov A.V. Estimates of variations in CO₂ radiative forcing in the last century and in future. // *Optika Atmosfery i Okeana*. 2019. V. 32. No. 10. P. 856-859 [in Russian].

**Thank you very much for
attention**

**Website of Atmospheric Remote
Sensing Laboratory:**

[http ://troll.phys.spbu.ru](http://troll.phys.spbu.ru)